Available online at www.sciencedirect.com

SciVerse ScienceDirect

journal homepage: www.elsevier.com/locate/he

Hydrogen production by steam reforming of dimethyl ether over ZnO–Al_2O_3 bi-functional catalyst

Mei Yang [a,b], *Yong Men* [a], *Shulian Li* [a], *Guangwen Chen* [a,*]

[a] *Dalian National Laboratory for Clean Energy, Dalian Institute of Chemical Physics, Chinese Academy of Sciences, 457 Zhongshan Road, Dalian 116023, China*

[b] *Graduate University, Chinese Academy of Sciences, Beijing 100049, China*

ARTICLE INFO

Article history:
Received 12 November 2011
Received in revised form
7 February 2012
Accepted 12 February 2012
Available online 13 March 2012

Keywords:
Dimethyl ether
H_2 production
Bi-functional catalyst
$ZnAl_2O_4$
Steam reforming

ABSTRACT

A series of ZnO–Al_2O_3 catalysts with various ZnO/(ZnO + Al_2O_3) molar ratios have been developed for hydrogen production by dimethyl ether (DME) steam reforming within microchannel reactor. The catalysts were characterized by N_2 adsorption-desorption, X-ray diffraction and temperature programmed desorption of NH_3. It was found that the catalytic activity was strongly dependent on the catalyst composition. The overall DME reforming rate was maximized over the catalyst with ZnO/(ZnO + Al_2O_3) molar ratio of 0.4, and the highest H_2 space time yield was 315 mol $h^{-1}\cdot kg_{cat}^{-1}$ at 460 °C. A bi-functional mechanism involving catalytic active site coupling has been proposed to account for the phenomena observed. An optimized bi-functional DME reforming catalyst should accommodate the acid sites and methanol steam reforming sites with a proper balance to promote DME steam reforming, whereas all undesired reactions should be impeded without sacrificing activity. This work suggests that an appropriate catalyst composition is mandatory for preparing good-performance and inexpensive ZnO–Al_2O_3 catalysts for the sustainable conversion of DME into H_2-rich reformate.

1. Introduction

Recently, steam reforming of dimethyl ether (DME) has attracted much attention to produce hydrogen for PEMFCs [1–5]. DME as a promising hydrogen carrier has various advantages, such as high H/C ratio, high energy density, innocuous nature and easy storage and transportation due to the similar physical properties to those of LPG and LNG. Generally, steam reforming of DME (Eq. (1)) is considered to proceed through two consecutive reactions, viz the first step of hydrolysis of DME (Eq. (2)) to form methanol over a solid acid catalyst followed by the second step of the steam reforming of methanol (MSR, Eq. (3)) to produce hydrogen over a steam reforming catalyst. Therefore, the steam reforming of DME usually proceeds over a bi-functional catalyst consisting of dual sites of acid sites and MSR sites.

DME steam reforming:

$$CH_3OCH_3 + 3H_2O(g) \rightarrow 2CO_2 + 6H_2, \quad \Delta H_R^o = 122 \text{ kJ/mol} \qquad (1)$$

DME hydrolysis:

$$CH_3OCH_3 + H_2O(g) \leftrightarrow 2CH_3OH(g), \quad \Delta H_R^o = 24 \text{ kJ/mol} \qquad (2)$$

Steam reforming of methanol (MSR):

$$CH_3OH(g) + H_2O(g) \rightarrow 3H_2 + CO_2, \quad \Delta H_R^o = 49 \text{ kJ/mol} \qquad (3)$$

Up to now, many catalysts have been developed for steam reforming of DME, which are usually in the form of the

* *Corresponding author*. Tel.: +86 411 84379301(Office); fax: +86 411 84379327.
E-mail address: gwchen@dicp.ac.cn (G. Chen).

0360-3199/$ – see front matter
doi:10.1016/j.ijhydene.2012.02.070

mechanical mixture of a solid acid and an MSR catalyst. Zeolite [6,7] and γ-Al_2O_3 [8,9] are two types of widely used solid acids. Other acidic catalysts studied also include WO_3–ZrO_2 [10] and ZrO_2 [11]. Cu-based catalyst is the common MSR catalyst due to the cost effectiveness and high activity [12,13]. The reaction mechanism and role of each component of Cu-based catalyst for MSR have been well studied [13,14]. When Cu-based catalyst is coupled with ZSM-5 with the Brønsted acid, DME steam reforming can proceed with a low CO selectivity below 300 °C [15]. Nonetheless, this composite catalyst is prone to deactivation due to the coke deposition. Al_2O_3 with weaker acid sites has been reported to be more durable for DME hydrolysis, but a relatively higher temperature between 350 °C and 500 °C is required for efficient hydrolysis of DME. From such a point of view, MSR following the hydrolysis of DME should be carried out above 350 °C to obtain a high overall DME reaction rate. Unfortunately, Cu-based catalysts such as Cu/ZnO/Al_2O_3 are easily deactivated due to the sintering of metallic Cu at this elevated temperature. Therefore, considerable effort has been made to get through this problem. There are mainly two solutions from a series of the open literatures dedicated to DME steam reforming. One is improving the thermal stability of metallic Cu by the formation of spinel oxide or alloy. Wang et al. found that the addition of Ni leaded to hindering sintering of Cu due to the promotion of Cu dispersion [16]. Cu–Ni/γ-Al_2O_3 catalyst showed a full DME conversion during the 30 h reaction time at 350 °C. Faungnawakij et al. developed the composite catalysts of $CuFe_2O_4$ coupled with γ-Al_2O_3, exhibiting good activity and stability in DME steam reforming in the temperature range of 350–450 °C [17–19]. The high dispersion of metallic copper in the matrix of iron oxides reduced from spinel structure and their strong chemical interaction were attributed to the excellent performance. The other is developing other active sites instead of Cu. Mathew et al. investigated the performance of Ga_2O_3–Al_2O_3 catalyst, which showed 100% DME conversion at 400 °C [20]. Solymosi et al. found Mo_2C/Norit + Al_2O_3 as an active catalyst above 380 °C [21]. However, the CO selectivity of these catalysts was a little high (Ga_2O_3–Al_2O_3, 54%; Mo_2C/Norit + Al_2O_3, 37%). To sum up, it is one of the interesting topics to develop a green, inexpensive and efficient Cu-free catalyst for DME steam reforming.

ZnO–Al_2O_3 as a catalyst support for noble metal or a catalyst has been widely used for oxidative dehydrogenation of 1-butene [22] and reverse water gas shift reaction [23]. It is also a very important component of Cu/ZnO/Al_2O_3 catalyst used in methanol synthesis and steam reforming [24]. In our previous work, we developed ZnO–Al_2O_3 (ZnO/(ZnO + Al_2O_3) $\geq$ 0.5) as an effective catalyst for high temperature MSR [25]. In spite of the vast amount of literatures published on catalytic transformation of methanol and its derivatives over ZnO–Al_2O_3 catalysts, their applications in DME reforming were rarely reported. Nilsson et al. found that a PdZn catalyst in which the support comprised mainly $ZnAl_2O_4$ exhibited improved activity compared to an Al_2O_3-supported PdZn catalyst in DME autothermal reforming [26]. In this paper, ZnO–Al_2O_3 catalysts (ZnO/(ZnO + Al_2O_3) $\leq$ 0.5), as Cu-free catalysts, have been developed for hydrogen production by steam reforming of DME. ZnO–Al_2O_3 catalysts provide dual active sites of acid sites and MSR sites in mutual interaction with atomic scale, resulting in a good-performance for DME steam reforming.

2. Experimental

2.1. Catalyst preparation

The catalysts were prepared by a co-precipitation method (for more details concerning the preparation, see [25]). Metal nitrates [$Zn(NO_3)_2 \cdot 6H_2O$, $Al(NO_3)_3 \cdot 9H_2O$] and aqueous ammonium with stoichiometric molar ratios were used as the starting materials. The process was operated at room temperature under vigorous stirring and the pH was kept at 7–8. The precipitate was aged in the mother liquid for 1 h, then removed, washed with de-ionized water several times and centrifuged. The obtained deposit was dried, calcined at 500 °C, and then grounded, pressed, crushed and screened to 40–60 mesh (0.245–0.35 mm). The resultant ZnO–Al_2O_3 samples are designated as ZnO-X, in which the symbol X represents the ZnO/(ZnO + Al_2O_3) molar ratio.

2.2. Catalyst characterization

The BET specific surface areas of the samples were measured by the BET method on an Auto Sorb iQ 2 instrument using nitrogen adsorption isotherms at 77 K.

The X-ray diffraction (XRD) patterns were obtained with a PANalytical X'Pert-Pro powder X-ray diffractometer, using Cu Kα monochromatized radiation (λ = 0.1541 nm) at a scan speed of 5°/min. The Spectra of the catalyst was collected after calcination.

Temperature programmed desorption of NH_3 (NH_3–TPD) was performed on a Micromeritics AutoChem 2920 apparatus. The amount of 200 mg catalyst was placed into a quartz U tube, heated for 1 h at 450 °C in Ar, and then kept at 100 °C for NH_3 adsorption. When saturated adsorption was achieved, the system was purged by He for 1 h. Then the temperature was programmed from 100 °C to 450 °C under the heating rate of 10 °C/min. The desorbed NH_3 was analyzed by a TCD detector.

2.3. Catalyst activity test

The steam reforming of DME was carried out in a multi-channel microreactor (see [25]) under atmospheric pressure. The microreactor has 10 parallel channels with a width of 1.5 mm, a depth of 1.5 mm and a length of 40 mm. 1 g catalyst particles with the size of 40–60 mesh were packed within the channels.

A mixture of DME, N_2 and water was purveyed into the vaporizer at 280 °C. The vapor was then fed into the microreactor. Subsequently, the reactor effluent passed through a condenser with a mixture of ice-water to trap the unreacted water. The dry reformate were analyzed by an on-line gas chromatograph (GC 4000A, Beijing East & West Analytical Instruments Inc) equipped with a thermal conductivity detector (TCD) and flame ionization detector (FID). A carbon molecular sieve column (TDX-01) was used to separate H_2, N_2, CO, CH_4 and CO_2 and a column of GDX-104 was used to detect

DME. The flow rate of the dry reformate was measured by a soap bubble flow meter. All the data were collected when the catalytic activity was kept stable, and material balances on N_2 was calculated to verify the measurement accuracy.

In this work, GHSV (calculated on the basis of the flow rate of DME and water under the conditions of 1 atm and 25 °C), DME conversion ($X_{DME,\ nominal}$), CO selectivity (S_{CO}) in dry reformate and H_2 space time yield (Y_{H_2}) are defined as the following:

$$GHSV = (Q_{DME} + Q_{H_2O})/V_R \times 60 \quad (4)$$

$$X_{DME,\ nominal} = n_{DME\ to\ H_2}/n_{DME,0} \times 100 = (n_{CO} + n_{CO_2} + n_{CH_4})/2n_{DME,0} \times 100 \quad (5)$$

$$S_{CO} = n_{CO}/(n_{CO} + n_{CO_2} + n_{CH_4}) \times 100 \quad (6)$$

$$Y_{H_2} = n_{H_2}/m_{cat} \times 60 \times 1000 \quad (7)$$

Where Q_{DME} and Q_{H_2O} are the gas flow rate of DME and water, ml min^{-1}; V_R is the microreactor's volume, ml; n_{CO}, n_{CO_2}, n_{CH_4} and n_{H_2} is the molar flow rate of CO, CO_2, CH_4 and H_2 in the dry reformate, mol/min; $n_{DME\ to\ H_2}$ is the molar ratio rate of DME which can be transformed to H_2, mol/min; $n_{DME,0}$ is the molar flow rate of DME in the feed, mol/min; m_{cat} is the weight of the catalyst, g.

3. Results and discussion

3.1. Catalyst characterization

3.1.1. The BET surface area and XRD results

The relation of the catalyst composition and BET surface area is summarized in Table 1. The BET surface area decreases monotonously with the increasing zinc content. Al_2O_3 maintains the largest surface area of 246 m^2/g. When the molar fraction of ZnO increases to 50%, the BET surface area decreases to 118 m^2/g.

Fig. 1 shows the XRD patterns of the samples with different zinc content. These patterns indicate a poor crystallinity for all samples. Our previous work showed that ZnO and Al_2O_3 can be easily transformed into zinc aluminate spinel once heated at 500 °C [25]. Hence, in the case of ZnO-50, ZnO-45, ZnO-40, ZnO-35 and ZnO-24, only the characteristic peaks of zinc aluminum spinel are observed. Furthermore, as shown in Fig. 1, the peaks of zinc aluminate spinel are found to move to the larger angle side with the decreasing zinc content. According to the literature, the excessive Al_2O_3 can be dissolved into the stoichiometric zinc aluminate spinel to form Al-rich non-stoichiometric spinel [27]. If Al-rich non-stoichiometric spinel is formed, the peaks of zinc aluminate spinel will move to the larger angle side due to the smaller size of Al^{3+} ions (Ionic radius of Al^{3+} ions in coordination 4 is 0.039 nm and that of Zn^{2+} ions is 0.060 nm [28]). In our study, it is indeed the case. This indicates that the excessive Al_2O_3 is dissolved into the stoichiometric zinc aluminate spinel (ZnO-50) to form Al-rich non-stoichiometric spinel for ZnO-45, ZnO-40, ZnO-35 and ZnO-24. In the Al-rich spinel, the Al^{3+} ions are present at both tetrahedral and octahedral sites, whereas the Al^{3+} ions exclusively locate at octahedral sites in stoichiometric spinel. However, the different coordination of Al^{3+} ions seems to have no obvious effect on the catalytic activity for DME steam reforming (as discussed in the following sections). The XRD pattern of Al_2O_3 displays three very broad peaks at $2\theta = 36.8°$, 45.7° and 66.4°, indicating the presence of poorly crystalline γ-Al_2O_3. Since γ-Al_2O_3 is of poor crystallization, the presence of γ-Al_2O_3 can not be clearly distinguished in ZnO-45, ZnO-40, ZnO-35 and ZnO-24.

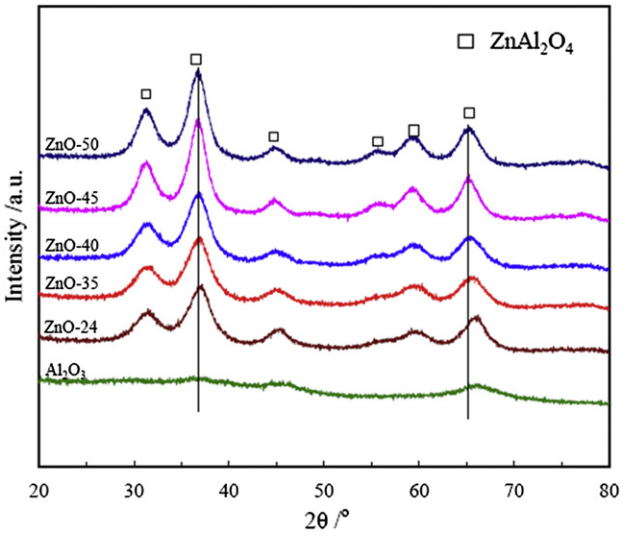

Fig. 1 – The XRD patterns of the samples with different zinc content. The XRD patterns of ZnO-50, ZnO-24 and Al_2O_3 have been reported in the reference [25].

Table 1 – The BET surface area of the catalysts with different zinc content[a].

Sample	Catalyst composition (mol%)		S_{BET} (m^2/g)
	ZnO	Al_2O_3	
Al_2O_3[a]	0	100	246
ZnO–24[a]	24	76	229
ZnO-35	35	65	207
ZnO-40	40	60	179
ZnO-45	45	55	141
ZnO–50[a]	50	50	118

a The BET surface area of Al_2O_3, ZnO-24 and ZnO-50 has been reported in reference [25].

3.1.2. The NH_3–TPD results

In the steam reforming of DME, the first step, DME hydrolysis, always occurs over the acid sites. The activity is strongly influenced by the amount and strength of acid sites. Faungnawakij et al. found that stronger acid sites are beneficial to the hydrolysis of DME [29]. In this paper, the surface acidity of all samples investigated was evaluated by NH_3–TPD, and the results are present in Fig. 2. It is well-known that a low/high NH_3 desorption temperature is related to weak/strong acid sites. Typically, three classes of acid sites are defined: weak

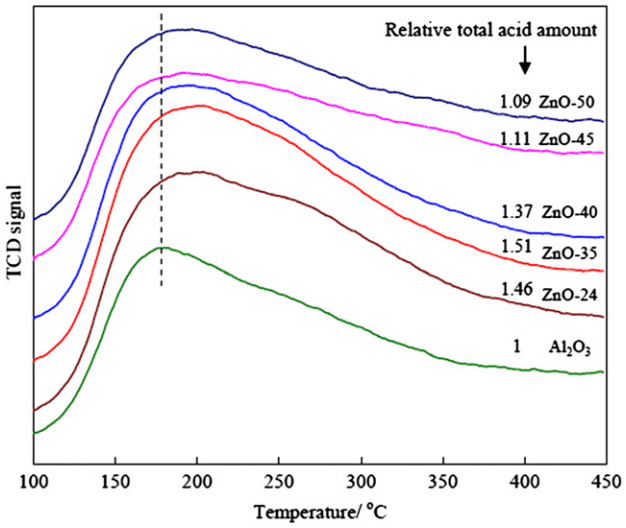

Fig. 2 – NH_3–TPD patterns of the samples with different zinc content.

(25–200 °C), intermediate (200–400 °C) and strong (>400 °C) [30]. As shown in Fig. 2, all samples display a broad peak originated from 100 °C to 450 °C, indicating all samples exhibit a broad distribution of acid strengths. The relative total acid amount of the samples investigated is also summarized in Fig. 2. Al_2O_3 has the smallest total acid amount with a peak temperature of 180 °C. By the incorporation with Zn, the peak temperature of Al_2O_3 shifts to 200 °C and the NH_3-uptake area increases, indicating the enhancement of both acid strength and total acid amount. With respect to the XRD results, it can be concluded that the formation of zinc aluminate spinel may be related to the increase in the acid amount and strength of Al_2O_3. This result is in accordance with Wrzyszcz et al.'s results that zinc aluminate spinel possessed higher total acid amount than Al_2O_3 [31]. Tanabe et al. also found the acid strength and amount of ZnO–Al_2O_3 varied with the composition and the maximum acid amounts were observed when the content of ZnO was 10% mol at any acid strength [32]. In this study, the relative total acid amount is found in the order as follows: ZnO-35 > ZnO-24 > ZnO-40 > ZnO-45 > ZnO-50 > Al_2O_3. It can be speculated that the catalytic activity of these samples for DME hydrolysis follow the similar trend.

3.2. *Catalytic activity for DME steam reforming*

3.2.1. *Effect of the catalyst composition*

The DME conversion is plotted in Fig. 3a as a function of the zinc content in the temperature range of 420–470 °C. The experiments were operated under the conditions of GHSV = 7900 h^{-1} and H_2O/DME = 4.8. It is observed that the DME conversion increases with the reaction temperature over all the samples investigated. Al_2O_3 alone does not show considerable activity within the temperature range studied for DME steam reforming ($X_{DME,\ nominal} \approx 5\%$, at 440 °C, not showed). As shown in Fig. 3a, incorporating Al_2O_3 with Zn enhances the catalytic activity of DME steam reforming dramatically. The overall DME conversion is 46.0%, 84.7%,

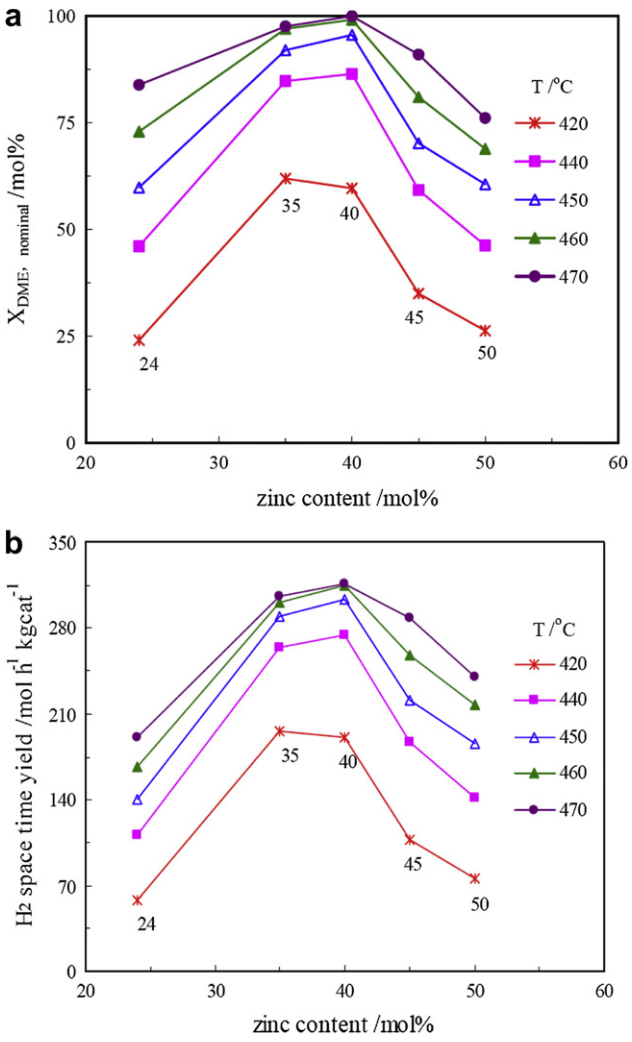

Fig. 3 – (a) The DME conversion and (b) The H_2 space time yield as a function of zinc content in the temperature range of 420–470 °C. GHSV = 7900 h^{-1}, H_2O/DME = 4.8.

86.4%, 59.2% and 46.2% over ZnO-24, ZnO-35, ZnO-40, ZnO-45 and ZnO-50 at 440 °C, respectively. As mentioned in the introduction, two reactions are mainly involved in the DME steam reforming: the hydrolysis of DME to methanol, which is catalyzed by acid sites; and the subsequent MSR. One can see that it is necessary to combine the acid sites and MSR sites with a proper balance to maximize the overall DME reaction rate. Generally, Al_2O_3 is well-known as a solid acid which can catalyze the hydrolysis of DME over 350 °C, while Zn^{2+} ions in zinc aluminate spinel are regarded as the active sites for MSR over 350 °C. It is evident that Al_2O_3 and Zn^{2+} ions in zinc aluminate spinel are active in the similar temperature region. Therefore, it is anticipated that ZnO–Al_2O_3 can serve as an active bi-functional catalyst for DME steam reforming. As expected, ZnO–Al_2O_3 samples indeed perform well in DME steam reforming. A bi-functional mechanism involving active site coupling is proposed to account for the observation. DME hydrolysis to methanol occurs over acid sites of Al^{3+} ions, and then methanol reformation to H_2 and CO_2 happens over different sites of Zn^{2+} ions nearby.

Moreover, it can be clearly seen from Fig. 3a that the catalytic activity is strongly dependent on the catalyst composition. The DME conversion increases with the increasing zinc content and reaches maximum over ZnO-35 and ZnO-40 samples. Further increase in the zinc content does not improve the catalytic activity. Instead, the DME conversion decreases dramatically. The order of the activity is ZnO-35 ≈ ZnO-40 > ZnO-45 > ZnO-50 ≈ ZnO-24. Though ZnO-24 exhibits the highest BET surface area in these samples, this catalyst shows the lowest activity, indicating that the BET surface area is not the dominant factor for catalytic activity. Actually, the DME steam reforming performance is directly related to the ratio of the acid sites to MSR sites in previous studies. For example, in the mechanically mixed composite catalysts such as $CuFe_2O_4$–Al_2O_3 composite catalyst, the catalytic activity was determined by the weight ratio of $CuFe_2O_4$ to Al_2O_3, whose optimized value was 1/1–2/1 [2]. In this study, we believe that such a trend of the catalytic activity over ZnO–Al_2O_3 samples is also closely correlated with the ratio of the acid sites to MSR sites. On one hand, our previous work suggested that the activity of MSR decreased with the decreasing zinc content with ZnO molar fraction below 50% [25]. It can be seen from Table 2 that the order of MSR activity coincides with this regularity. That is ZnO-50 > ZnO-35 > ZnO-24. On the other hand, the acidy of the samples nearly follows the inverse trend (Fig. 2), indicating that the activity for DME hydrolysis increases with the decreasing zinc content. Therefore, to obtain a high overall DME conversion, the proper balance of acid sites and MSR sites must be matched. ZnO-40 and ZnO-35 with the highest DME conversion imply that these samples have the appropriate ratio of the acid sites to MSR sites. It can be concluded that the catalysts with ZnO/(ZnO + Al_2O_3)> 0.4 are in shortage of acid sites and the rate limiting step is the hydrolysis of DME under this operating condition, whereas the catalysts with ZnO/(ZnO + Al_2O_3) < 0.35 run short of MSR sites and the rate limiting step is MSR. Compared the results of MSR with those of DME steam reforming over ZnO-50 and ZnO-24, this conclusion is more obvious. It can be seen from Fig. 3a that ZnO-50 and ZnO-24 have the similar activity with DME conversion of 46% at 440 °C. However, the methanol conversion over ZnO-50 is 100% during MSR. This result strongly suggests that ZnO-50 is in shortage of the acid sites and the rate limiting step is the hydrolysis of DME (the relative acid amount is 1.09, Fig. 2). On the contrary, the methanol conversion is the same as DME conversion over ZnO-24 (the relative acid amount is 1.46, Fig. 2), indicating that the rate limiting step is switched to MSR for ZnO-24.

The H_2 space time yield is plotted in Fig. 3b. The H_2 space time yield increases with the reaction temperature due to the increase in DME conversion. ZnO-40 has the highest H_2 space time yield of 315 mol $h^{-1}\cdot kg_{cat}^{-1}$ at 460 °C. The H_2 space time yield of ZnO-50 is higher than that of ZnO-24, although they have the similar DME conversion. This is caused by the higher CO selectivity of ZnO-24, which will be shown in next paragraph.

The desired DME steam reforming to produce hydrogen proceeds by MSR to produce CO_2, while this reaction is always accompanied by other undesired reactions such as the decomposition of DME (Eq. (8)), reverse water gas shift reaction (RWGS, Eq. (9)) and decomposition of methanol (DM, Eq. (10)) with the formation of by-product CO. Fig. 4 displays the CO selectivity of all the samples investigated as a function of zinc content over the temperature range of 420–470 °C. It is evident that CO selectivity increases with both the increasing reaction temperature and the decreasing zinc content. Especially, the CO selectivity of ZnO-24 is far higher than those of other samples.

Decomposition of DME:

$$CH_3OCH_3 \rightarrow H_2 + CO + CH_4, \quad \Delta H_R^o = -1.0 \text{ kJ/mol} \tag{8}$$

RWGS:

$$CO_2 + H_2 \leftrightarrow H_2O(g) + CO, \quad \Delta H_R^o = 40 \text{ kJ/mol} \tag{9}$$

DM:

$$CH_3OH(g) \rightarrow 2H_2 + CO, \quad \Delta H_R^o = 90 \text{ kJ/mol} \tag{10}$$

3.2.2. *Reaction pathways over ZnO–Al_2O_3 catalysts*

Fig. 5 shows the product distribution of the dry reformate at 440 °C over all samples. It can be seen that the formation of CH_4 is below the detectable limit of GC over ZnO-50, ZnO-45

Table 2 – The results of MSR, DM, and CO methanation at 440 °C.

Reaction[a,b]	Sample	X_{MeOH} or X_{CO}/mol%	S_{CO}/mol%	S_{CH_4}/mol%	S_{CO_2}/mol%
Methanol decomposition	ZnO-50	70.7	72.9	2.5	24.6
	ZnO-35	87.3	59.0	14.5	26.4
	ZnO-24	86.1	49.7	24.8	25.5
	Al_2O_3	17.2	37.3	47.7	15.1
MSR	ZnO-50	100.0	5.7	0.0	94.3
	ZnO-35	88.5	10.7	0.4	88.9
	ZnO-24	45.3	41.8	9.0	49.2
	Al_2O_3	5.7	37.0	35.9	27.1
CO methanation	ZnO-24	0.2	–	–	–
	Al_2O_3	0.2	–	–	–

a Methanol conversion of decomposition and steam reforming was 3.3% and 1.3% in the blank test.
b MSR: $GHSV_{(MeOH)}$ = 2720 h^{-1}, H_2O/MeOH = 1.9; Methanol decomposition: $GHSV_{(MeOH)}$ = 2720 h^{-1}; CO methanation: $GHSV_{(CO)}$ = 909 h^{-1}, H_2/CO = 1.2.

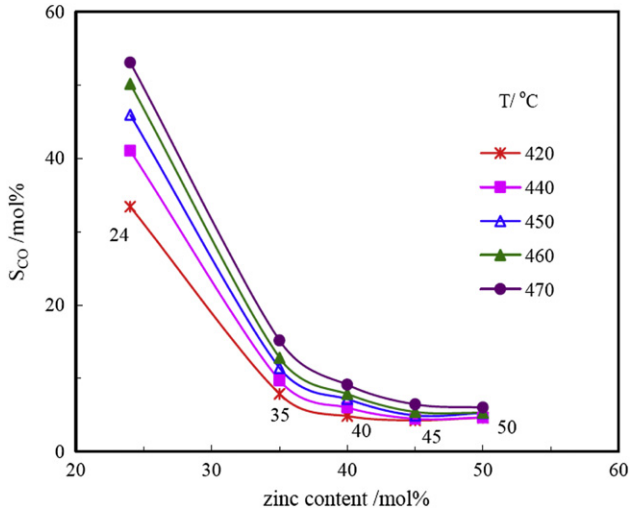

Fig. 4 – The CO selectivity as a function of zinc content in the temperature range of 420–470 °C. GHSV = 7900 h^{-1}, H_2O/DME = 4.8.

and ZnO-40. This indicates that the decomposition of DME can be ignored over these samples. ZnO-35 and ZnO-24 are found to produce CH_4, and the concentration of CH_4 is 0.04% and 2.92%, respectively. It is noticeable that the ratio of CO to CH_4 over these two samples is much larger than 1 (72 over ZnO-35; 4 over ZnO-24). This implies that CO is mainly not generated by the decomposition of DME. Thereby, the majority of by-product CO is formed via the methanol steam reforming process.

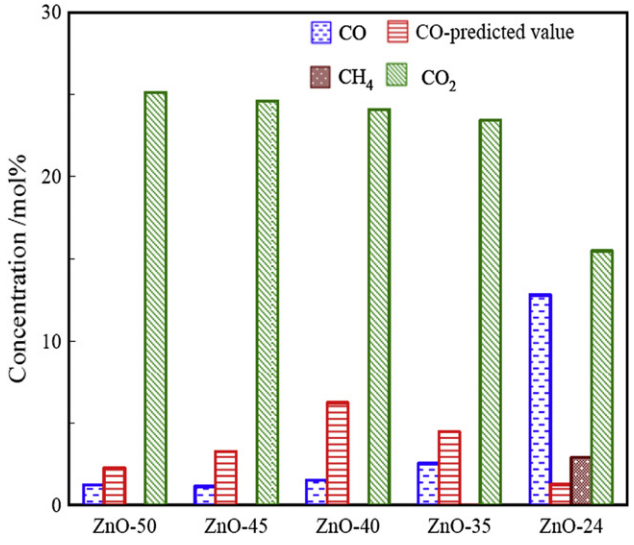

Fig. 5 – Concentration of CO, CH_4 and CO_2 in the product gas over the samples with different zinc content. Reaction temperature = 440 °C, GHSV = 7900 h^{-1}, H_2O/DME = 4.8. The 'CO-predicted value' was calculated on the assumption that methanol steam reforming proceeded via methanol decomposition followed by water gas shift reaction.

In order to shed light on the reaction pathway for CO and CH_4 production, methanol decomposition and steam reforming were carried out over selected ZnO–Al_2O_3 samples. The results are summarized in Table 2.

3.2.2.1. *Methanol decomposition (DM)*. As shown in Table 2, the methanol conversion is 17.2% over Al_2O_3, indicating that Al^{3+} ions can catalyze DM, even though the activity is very low. According to the literature, Zn^{2+} ions are active for DM [33]. Hence, DM on ZnO-50, ZnO-35 and ZnO-24 outperform that on Al_2O_3. In this paper, the methanol conversion is calculated on the basis of the carbon species in the gas product. There is severe carbon deposition over ZnO-50 and ZnO-35 samples, which become very dark after catalytic activity test. Therefore, the methanol conversion of ZnO-50 and ZnO-35 does not reach 100%, although there is no unreacted methanol condensed after the microreactor. It can be seen from Table 2 that CO selectivity decreases gradually with the decreasing zinc content, whereas CH_4 selectivity increases with the decrease in zinc content. Al_2O_3 has the lowest CO selectivity of 37.3% and highest CH_4 selectivity of 47.7%. This indicates that Zn^{2+} ions are more selective to CO than Al^{3+} ions in the absence of water, and the formation of CH_4 is brought about by the presence of Al^{3+} ions. Generally, CH_4 is a common by-product in methanol decomposition. The possible routes of CH_4 formation are stated as follows (Eqs. (11)–(13)) [34–36]. As shown in Table 2, it is evident that the methanation of CO can hardly proceed over ZnO-24 and Al_2O_3. Therefore, Eqs. (12) and (13) may contribute to the formation of CH_4 in DM.

$$CO + 3H_2 \rightarrow CH_4 + H_2O \quad (11)$$

$$CH_3OH + H_2 \rightarrow CH_4 + H_2O \quad (12)$$

$$2CH_3OH \leftrightarrow CH_3OCH_3 + H_2O,\ CH_3OCH_3 \rightarrow CO + CH_4 + H_2O \quad (13)$$

3.2.2.2. *Methanol steam reforming (MSR)*. When steam is added, one can see that there is a significant decline in CO selectivity over the selected ZnO–Al_2O_3 samples. For example, in the case of ZnO-50, the CO selectivity decreases from 72.9% to 5.7% with the addition of water. Some researchers suggested that water and methanol compete for the same adsorption sites over ZnO [37]. In the absence of water, methanol forms methoxy groups as intermediates, which can quickly be decomposed into H_2 and CO. When water is added, the methoxy groups are oxidated to formate groups, which can be decomposed into H_2 and CO_2. Accordingly, Zn^{2+} ions are more selective to CO_2 than CO in the presence of water. Furthermore, it is evident in Table 2 that the CO selectivity goes up with the decreasing zinc content during MSR. This trend is similar with that of the CO selectivity during DME steam reforming, indicating that CO is indeed formed via the methanol steam reforming process.

Initially, CO is regarded as an intermediate and formed directly through DM followed by water gas shift reaction (WGS) during MSR [38]. However, this mechanism becomes unacceptable since many results have shown that the CO level in the reformate gas is dramatically lower than the predicted value from WGS equilibrium [39]. This conclusion is reconfirmed in

our study. The predicted value of CO has been calculated on the assumption that MSR proceeds via DM followed by WGS. Since WGS is limited by the thermodynamic equilibrium, the predicted value of CO represents the minimal CO concentration which can be obtained on the basis of this mechanism. As shown in Fig. 5, it is evident that the CO concentration in the steam reforming process was below the predicted value from WGS equilibrium over all samples except ZnO-24. This indicates that MSR does not proceed via DM/WGS sequential route. As mentioned in our previous work [25], the side reactions, RWGS and DM, were both responsible for the formation of CO over ZnO–Al_2O_3 catalysts. For ZnO-24, the CO concentration was higher than the equilibrium value. The result implied that methanol steam reforming, the second step in DME steam reforming, followed a methanol decomposition/WGS sequential route or methanol steam reforming/methanol decomposition parallel route. Subsequently, WGS was conducted under the reaction conditions similar to the outlet composition of the steam reforming based on the assumption that CO_2 in the steam reforming was produced through WGS over ZnO-24. However, the CO_2 concentration after WGS was much lower than that of the steam reforming process (the CO conversion was only 4.9% in WGS process), indicating that CO was mainly generated by methanol decomposition over ZnO-24. In the case of Al_2O_3, one can see that the CO selectivity is nearly the same in DM and MSR. This indicates that Al^{3+} ions are only active for DM even in the presence of water. These results suggest that more methanol molecules decompose to CO and H_2 with the increasing Al content in the presence of water, causing the CO selectivity to go up with the increase in Al content.

To sum up, the methanol produced by the hydrolysis of DME is mainly transformed to H_2 and CO_2 during DME steam reforming. In parallel with this route, some methanol is directly decomposed to CO and H_2. In the presence of water, a higher Al content favors higher methanol decomposition. For the sample with zinc content lower than 35%, CH_4 becomes to be detectable in DME steam reforming. As shown in Table 2, the formation of CH_4 also occurs over these samples in MSR. As a consequence, CH_4 may be produced via DME decomposition paralleled with DME steam reforming or in MSR process.

3.2.3. *Effect of the molar ratio of water to DME (H_2O/DME)*

The effect of the molar ratio of H_2O/DME on the DME conversion and CO selectivity was investigated over ZnO-40. The experiments were carried out at 440 °C. It is evident in Fig. 6 that the DME conversion decreases with the increasing molar ratio of H_2O/DME, corresponding to a decrease in the CO selectivity. As the molar ratio of H_2O/DME increases from 3.7 to 6.7, the DME conversion and CO selectivity decrease from 92.3% to 74.4% and 9.3%–5.6%, respectively. In this work, Zn^{2+} ions act as the active component for methanol steam reforming. As mentioned above, some researchers suggest that water and methanol compete for the same adsorption sites on ZnO. Therefore, the rising water reduces the coverage of absorptive methanol, leading to a decrease in the MSR rate. On the other hand, since Lewis acid sites and MSR sites coexist over ZnO-40, it is impossible to investigate the effect of the molar ratio of H_2O/DME on DME hydrolysis experimentally over ZnO-40. Therefore, DME hydrolysis was carried out over

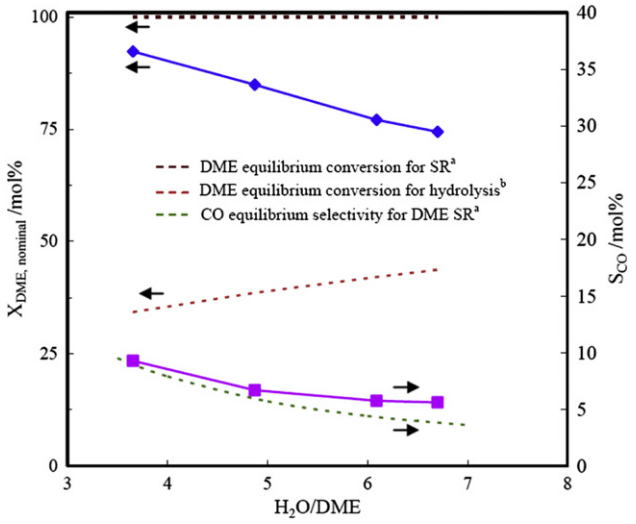

Fig. 6 – The DME conversion and CO selectivity as a function of H_2O/DME ratio over ZnO-40. Reaction temperature = 440 °C [a]The equilibrium value of X_{DME} and S_{CO} for DME SR was adopted from [40]; [b]The equilibrium value of X_{DME} for DME hydrolysis was calculated by the Gibbs free energy minimization method.

Al_2O_3, and the results are summarized in Table 3. As shown in Table 3, DME conversion approaches to the thermodynamic equilibrium even at the molar ratio of H_2O/DME as high as 7, indicating that there are sufficient acid sites over Al_2O_3 to catalyze DME hydrolysis. Furthermore, it is evident that DME hydrolysis is promoted by the increasing molar ratio of H_2O/DME. On the basis of the NH_3-TPD results, the relative total acid amount of ZnO-40 is larger than that of Al_2O_3. It can be predictable that the thermodynamic equilibrium of DME hydrolysis will move to the right with the increasing molar ratio of H_2O/DME over ZnO-40. In summary, the effect of the increasing molar ratio of H_2O/DME mainly embodies in two aspects: (1) promote the DME hydrolysis; (2) restrain the methanol steam reforming. According to the literature, the DME conversion is determined by both DME hydrolysis rate and MSR rate [2]. Hence, the DME conversion may go up, or may decline with the increasing H_2O/DME ratio. At the moment, the DME conversion decreases gradually with the increasing molar ratio of H_2O/DME, indicating that the promotion effect on the hydrolysis of DME can not offset the inhibition effect on MSR.

3.2.4. *Life time*

At last, the durability of ZnO-40 catalyst was investigated under the reaction conditions of 440 °C, GHSV = 7900 h^{-1} and

Table 3 – DME conversion at different molar ratios of H_2O/DME for DME hydrolysis over Al_2O_3 at 440 °C.

H_2O/DME	X_{DME}/%	X_{DME}-equilibrium/%
4.8	39.5	38.8
7.0	46.7	45.0

H_2O/DME = 4.8. As shown in Fig. 7, there is no significant deactivation of ZnO-40 catalyst over 50 h continuous operation. In the entire run of time on stream, the conversion of DME remains above 83%, and the H_2 space time yield is above 260 mol h^{-1} kg_{cat}^{-1}. Noticeably, the CO selectivity increased gradually from 6.0% to 8.5%. This may be caused by the instability of Al-rich non-stoichiometric spinel under the reaction condition. To validate this hypothesis, we further investigated the stability of ZnO-50 (stoichiometric spinel). To keep the DME conversion above 80%, this test was carried out at 460 °C and GHSV of 4760 h^{-1}. It can be seen from Fig. 8 that the catalyst is stable in the 100 h test with a constant CO selectivity of 8.5%. However, the exact nature of the instability of Al-rich non-stoichiometric spinel remains unclear on the basis of our results, and needs further investigation.

The catalyst structure of ZnO-40 and ZnO-50 after the durability test was examined by XRD. As shown in Fig. 9, the XRD patterns of ZnO-50 and ZnO-40 after reaction is sharpened to some extent. Crystalline of zinc aluminate spinel

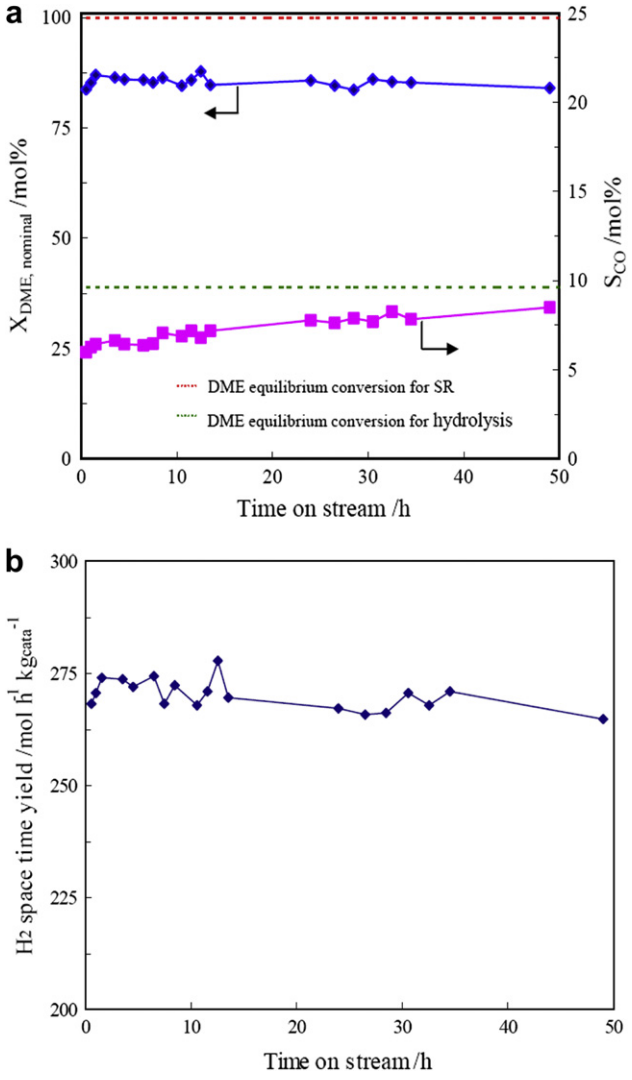

Fig. 7 – (a) Stability test (b) H_2 space time yield over ZnO-40 catalyst. Reaction temperature = 440 °C, GHSV = 7900 h^{-1}, H_2O/DME = 4.8.

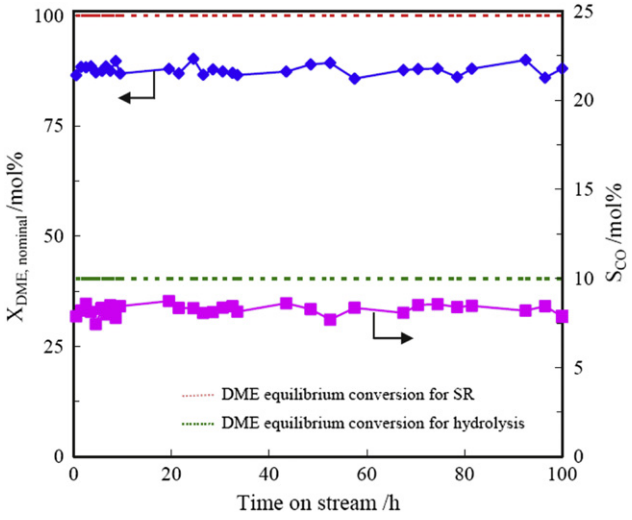

Fig. 8 – Stability test over ZnO-50 catalyst. Reaction temperature = 460 °C, GHSV = 4760 h^{-1}, H_2O/DME = 4.8.

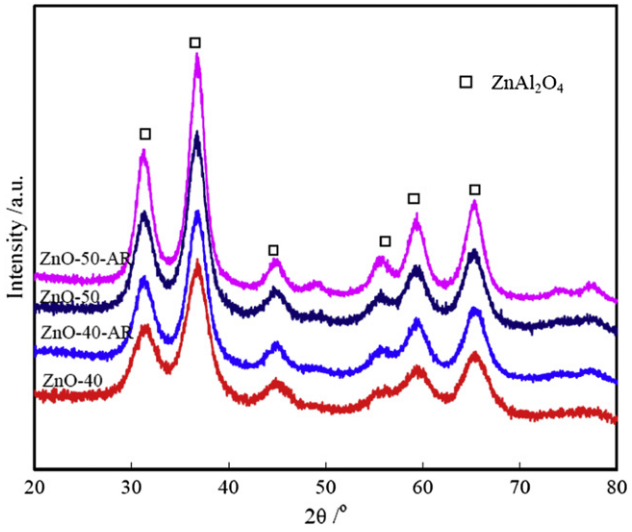

Fig. 9 – XRD patterns of ZnO-40 and ZnO-50 after reaction.

increased from 3.8 nm to 4.9 nm and 3.2 nm–3.8 nm for ZnO-50 and ZnO-40, respectively. However, this increase in crystalline does not result in any noticeable deactivation in the catalytic activity.

4. Conclusion

In this study, a series of ZnO–Al_2O_3 samples prepared by co-precipitation method are demonstrated as efficient catalysts for DME steam reforming. The bi-functionality of the ZnO–Al_2O_3 accommodating the acid sites formed by Al^{3+} ions and the MSR sites of Zn^{2+} ions was found to be responsible for the excellent performance for DME steam reforming. To obtain a high DME overall conversion, the proper balance of surface acid sites and MSR sites had to be obtained over optimized

catalyst, and turning the ZnO/(ZnO + Al_2O_3) molar ratio could find an appropriate catalyst composition to meet this requirement. It was proposed that the composition of the binary metal oxide played a crucial role in promoting DME steam reforming and suppressing side reactions, such as the methanation and decomposition. The samples with optimized ZnO/(ZnO + Al_2O_3) molar ratio between 0.4 and 0.5 exhibited the best performance.

The CO selectivity was found to increase with the increasing Al content. During DME steam reforming, the methanol produced by the hydrolysis of DME was mainly transformed to H_2 and CO_2. In parallel, some methanol was directly decomposed to CO and H_2. In the presence of water, a higher Al content favored higher methanol decomposition rate. CH_4 may be produced via DME decomposition paralleled with DME steam reforming or in MSR process.

At last, the life test was carried out to check the stability of ZnO-40 and ZnO-50. During the test, there was no obvious deactivation over these samples. Considering the easy availability and low cost of ZnO–Al_2O_3, the present catalyst system can serve as a potential bi-functional and inexpensive metal oxide catalyst for steam reforming of DME.

Acknowledgment

The authors gratefully acknowledge the financial support of the DICP 100-Talent Program, the Natural Science Foundation of Liaoning Province (201102219), and the National Natural Science Foundation of China (No. 20906087).

REFERENCES

[1] Galvita VV, Semin GL, Belyaev VD, Yurieva TM, Sobyanin VA. Production of hydrogen from dimethyl ether. Appl Catal A 2001;216:85–90.
[2] Tanaka Y, Kikuchi R, Takeguchi T, Eguchi K. Steam reforming of dimethyl ether over composite catalysts of gamma-Al_2O_3 and Cu-based spinel. Appl Catal B 2005;57:211–22.
[3] Mathew T, Yamada Y, Ueda A, Shioyama H, Kobayashi T. Metal oxide catalysts for DME steam reforming: Ga_2O_3 and Ga_2O_3-Al_2O_3 catalysts with and without copper. Appl Catal A 2005;286:11–22.
[4] Eguchi K, Faungnawakij K, Fukunaga T, Kikuchi R. Deactivation and regeneration behaviors of copper spinel-alumina composite catalysts in steam reforming of dimethyl ether. J Catal 2008;256:37–44.
[5] Park S, Choi B, Oh BS. A combined system of dimethyl ether (DME) steam reforming and lean NO_x trap catalysts to improve NO_x reduction in DME engines. Int J Hydrogen Energy 2011;36:6422–32.
[6] Matsumoto T, Nishiguchi T, Kanai H, Utani K, Matsumura Y, Imamura S. Steam reforming of dimethyl ether over H-mordenite-Cu/CeO_2 catalysts. Appl Catal A 2004;276:267–73.
[7] Shimoda N, Faungnawakij K, Kikuchi R, Eguchi K. A study of various zeolites and $CuFe_2O_4$ spinel composite catalysts in steam reforming and hydrolysis of dimethyl ether. Int J Hydrogen Energy 2011;36:1433–41.
[8] Faungnawakij K, Shimoda N, Fukunaga T, Kikuchi R, Eguchi K. Cu-based spinel catalysts CuB_2O_4 (B = Fe, Mn, Cr, Ga, Al, $Fe_{0.75}Mn_{0.25}$) for steam reforming of dimethyl ether. Appl Catal A 2008;341:139–45.
[9] Faungnawakij K, Shimoda N, Fukunaga T, Kikuchi R, Eguchi K. Crystal structure and surface species of $CuFe_2O_4$ spinel catalysts in steam reforming of dimethyl ether. Appl Catal B 2009;92:341–50.
[10] Oka K, Nishiguchi T, Kanai H, Utani K, Imamura S. Active state of tungsten oxides on WO_3/ZrO_2 catalyst for steam reforming of dimethyl ether combined with CuO/CeO_2. Appl Catal A 2006;309:187–91.
[11] Llorca J, Ledesma C, Ozkan US. Hydrogen production by steam reforming of dimethyl ether over Pd-based catalytic monoliths. Appl Catal B 2011;101:690–7.
[12] Turco M, Bagnasco G, Cammarano C, Micoli L, Lenarda M, Moretti E, et al. The role of H_2O and oxidized copper species in methanol steam reforming on a Cu/CeO_2/Al_2O_3 catalyst prepared by one-pot sot-gel method. Appl Catal B 2011;102:387–94.
[13] Jones SD, Hagelin-Weaver HE. Steam reforming of methanol over CeO_2- and ZrO_2-promoted Cu-ZnO catalysts supported on nanoparticle Al_2O_3. Appl Catal B 2009;90:195–204.
[14] Kurr P, Kasatkin I, Girgsdies F, Trunschke A, Schlögl R, Ressler T. Microstructural characterization of Cu/ZnO/Al_2O_3 catalysts for methanol steam reforming - A comparative study. Appl Catal A 2008;348:153–64.
[15] Kawabata T, Matsuoka H, Shishido T, Li DL, Tian Y, Sano T, et al. Steam reforming of dimethyl ether over ZSM-5 coupled with Cu/ZnO/Al_2O_3 catalyst prepared by homogeneous precipitation. Appl Catal A 2006;308:82–90.
[16] Wang XL, Pan XM, Lin R, Kou SY, Zou WB, Ma JX. Steam reforming of dimethyl ether over Cu-Ni/gamma-Al_2O_3 bi-functional catalyst prepared by deposition-precipitation method. Int J Hydrogen Energy 2010;35:4060–8.
[17] Faungnawakij K, Tanaka Y, Shimoda N, Fukunaga T, Kikuchi R, Eguchi K. Hydrogen production from dimethyl ether steam reforming over composite catalysts of copper ferrite spinel and alumina. Appl Catal B 2007;74:144–51.
[18] Faungnawakij K, Shimoda N, Viriya-empikul N, Kikuchi R, Eguchi K. Limiting mechanisms in catalytic steam reforming of dimethyl ether. Appl Catal B 2010;97:21–7.
[19] Faungnawakij K, Kikuchi R, Fukunaga T, Eguchi K. Stability enhancement in Ni-Promoted Cu-Fe spinel catalysts for dimethyl ether steam reforming. J Phys Chem C 2009;113:18455–8.
[20] Mathew T, Yamada Y, Ueda A, Shioyama H, Kobayashi T. Metal oxide catalysts for DME steam reforming: Ga_2O_3 and Ga_2O_3-Al_2O_3 catalysts. Catal Lett 2005;100:247–53.
[21] Solymosi F, Barthos R, Kecskeméti A. The decomposition and steam reforming of dimethyl ether on supported Mo_2C catalysts. Appl Catal A 2008;350:30–7.
[22] Toledo JA, Bosch P, Valenzuela MA, Montoya A, Nava N. Oxidative dehydrogenation of 1-butene over Zn-Al ferrites. J Mol Catal A 1997;125:53–62.
[23] Park SW, Joo OS, Jung KD, Kim H, Han SH. Development of ZnO/Al_2O_3 catalyst for reverse-water-gas-shift reaction of CAMERE (carbon dioxide hydrogenation to form methanol via a reverse-water-gas-shift reaction) process. Appl Catal A 2001;211:81–90.
[24] Baltes C, Vukojevic S, Schuth F. Correlations between synthesis, precursor, and catalyst structure and activity of a large set of CuO/ZnO/Al_2O_3 catalysts for methanol synthesis. J Catal 2008;258:334–44.
[25] Yang M, Li SL, Chen GW. High-temperature steam reforming of methanol over ZnO-Al_2O_3 catalysts. Appl Catal B 2011;101:409–16.
[26] Nilsson M, Jansson K, Jozsa P, Pettersson LJ. Catalytic properties of Pd supported on ZnO/$ZnAl_2O_4$/Al_2O_3 mixtures

in dimethyl ether autothermal reforming. Appl Catal B 2009; 86:18–26.
[27] van der Laag NJ, Snel MD, Magusin PCMM, de With G. Structural, elastic, thermophysical and dielectric properties of zinc aluminate ($ZnAl_2O_4$). J Eur Ceram Soc 2004;24:2417–24.
[28] Shannon RD. Revised effective ionic-radii and systematic studies of interatomic distances in halides and chalcogenides. Acta Crystallogr A 1976;32:751–67.
[29] Faungnawakij K, Tanaka Y, Shimoda N, Fukunaga T, Kawashima S, Kikuchi R, et al. Influence of solid-acid catalysts on steam reforming and hydrolysis of dimethyl ether for hydrogen production. Appl Catal A 2006;304:40–8.
[30] Maciver DS, Tobin HH, Barth RT. Catalytic alumina I: surface chemistry of eta and gamma-alumina. J Catal 1963;2:485–97.
[31] Wrzyszcz J, Zawadzki M, Trawczynski J, Grabowska H, Mista W. Some catalytic properties of hydrothermally synthesised zinc aluminate spinel. Appl Catal A 2001;210:263–9.
[32] Shibata K, Kiyoura T, Kitagawa J, Sumiyosh T, Tanabe K. Acidic properties of binary metal-oxides. Bull Chem Soc Jpn 1973;46:2985–8.
[33] Tawarah KM, Hansen RS. Kinetics and mechanism of methanol decomposition over zinc oxide. J Catal 1984;87: 305–18.
[34] Solymosi F, Revesz K. Thermal stability of the methyl group adsorbed on the palladium (100) surface. J Am Chem Soc 1991;113:9145–7.
[35] Chang FW, Yu HY, Roselin LS, Yang HC. Production of hydrogen via partial oxidation of methanol over Au/TiO_2 catalysts. Appl Catal A 2005;290:138–47.
[36] Shishido T, Sameshima H, Takehira K. Methanol decomposition to synthesis gas over supported Pd catalysts prepared from hydrotalcite precursors. Top Catal 2003;22: 261–9.
[37] Chadwick D, Zheng KG. The importance of water in the mechanism of methanol decomposition on ZnO. Catal Lett 1993;20:231–42.
[38] Peters R, Dusterwald HG, Hohlein B. Investigation of a methanol reformer concept considering the particular impact of dynamics and long-term stability for use in a fuel-cell-powered passenger car. J Power Sources 2000;86:507–14.
[39] Breen JP, Meunier FC, Ross JRH. Mechanistic aspects of the steam reforming of methanol over a $CuO/ZnO/ZrO_2/Al_2O_3$ catalyst. Chem Comm; 1999:2247–8.
[40] Semelsberger TA, Borup RL. Thermodynamic equilibrium calculations of dimethyl ether steam reforming and dimethyl ether hydrolysis. J Power Sources 2005;152:87–96.